Take-Off and Landing Performance of Tactical UAV

Miodrag Milenković-Babić[1]
Dušan Ivković[1]
Branislav Ostojić[1]
Milenko Trifković[1]
Vuk Antonić[1]

The research presented in this paper focuses on take-off and landing performance of a single pusher-propelled Tactical unmanned aerial vehicle. The analysis presented includes flight test verification of estimated UAV characteristics. The study proposes a possible approximated method for estimating UAV characteristics. Flight test results have been conducted to verify the estimated results, and the calculated and measured results show good agreement.

Key words: **UAV, performance, flight tests results.**

Introduction

UNMANNED aerial vehicles (UAVs) must comply with regulatory criteria [1-3]. The estimation of UAV characteristics typically begins with analyzing the most important maneuver that the aircraft or UAV needs to accomplish: the take-off. It is crucial for designers to understand not only the take-off capabilities of the new design but also its limitations and sensitivity. Take-off performance primarily refers to the distance required for the aircraft or UAV to accelerate from a standstill to lift-off, as well as the distance required to attain an initial and steady climb. For UAVs, it's essential to ensure that they can be controlled safely and precisely by flight control operators. During the flight, a flight control computer manipulates the UAV, and flight control operators only need to define operational mission requirements such as desired flight path, altitude, and airspeed.

Regulatory requirements for UAV aerodynamic characteristics are usually confirmed by flight tests. These tests involve trying out many different configurations, including aborted take-off cases, the maximum allowed crosswind limits, the influence of the wet/ice runway, and all possible landing configurations. Such tests should be conducted at various altitudes, masses, environmental temperatures, and humidity, as defined in the regulations [1-3]. Take-off and landing performance are influenced by many factors that cannot be predicted or measured accurately. Ground effects on the aerodynamic transient processes in the terminal phase of flight, different autopilot flight control optimization, air density in different regions, and other factors affect these flight phases. To develop and validate reliable design estimation techniques for these performances, it is necessary to solve the complex problem and its sensitivity to different autopilot flight control optimizations. Estimation of UAV's capabilities is typically made within broad limits, based on statistical and error evaluations.

The mechanics of flight provides equations of motion for estimating take-off and landing performance [4]. A general methodology for conducting a fast and reliable study of these characteristics in conceptual design is presented in [5-6]. These nonlinear equations of motion can be solved numerically by computers. This research proposes an approximated numerical procedure for estimating take-off and landing performance based on the data given in [6].

The data from [6] provides a few methods that can be used for estimating take-off characteristics. The method used in this paper is specifically useful for the typical piston-engine aircraft or UAV as is Tactical UAV given in Fig.1. The Tactical UAV geometry is given in Table 1. In order to correctly predict UAV characteristics, it is necessary to obtain the precise value of the propeller efficiency factor. Estimation of the just-mentioned factor is a hard and very complex task during the preliminary UAV design phase. During this phase of UAV development, the propeller characteristics are usually not well known. More information will be given in the presented paper. As given in [6], when the propeller efficiency is not known, the estimated value should be:

- for fixed pitch climb propeller

$$\eta_{propeller} = 0.45 - 0.50,$$

- for fixed pitch cruise propeller

$$\eta_{propeller} = 0.35 - 0.45 \text{ and}$$

- for constant speed propeller

$$\eta_{propeller} = 0.45 - 0.60.$$

[1] Military Technical Institute (VTI), Ratka Resanovića 1, 11132 Belgrade, SERBIA
Correspondence to: Miodrag Milenković-Babić; e-mail: miodragmbm@yahoo.co.uk

Figure 1. Tactical UAV [6]

Table 1. UAV geometry

Tactical UAV	
Wing span (with winglet)	7.025 m
Wing aspect ratio	9.08
Length	5.556 m
Mean aerodynamic chord	0.736 m
Wing area	4.33 m^2
Engine power	38.8 KW
Propeller diameter	0.86 m
Maximal mass of UAV	265 kg

The just mentioned information is the most accurate estimation of the propeller efficiency in the preliminary design phase. All these uncertainties can have an impact on the calculated results for UAV performance, which can then be compared to flight test results. Even today, software solutions are being developed to estimate take-off and landing characteristics, such as those found in [7-9].

The Tactical UAV was designed according to military requirements. It is a remotely piloted aircraft that can carry different payloads, including communications equipment, sensors, cameras, missiles, etc. A method for estimating the performance of medium-range unmanned aerial vehicles with piston engines is presented in [10]. The major obstacles in developing and validating reliable UAV designs are primarily the complexity of the problem, the constantly changing requirements, and the ongoing improvements in available technology during the UAV development phase. As can be seen from the initial UAV data given in [10] and the data presented in Table 1, the maximum UAV mass increased, which caused a change in wing geometry and installed engine. The Tactical UAV was developed by the Military Technical Institute (VTI) in Belgrade.

Take-off distance

According to the regulation requirements that are given in [1], take-off and landing distance is precisely defined. For example, the take-off distance is defined as the horizontal distance that aircraft or UAV covered from brake release to clearing an obstacle at a height of 15 m above the runway. This horizontal distance must be determined for all weights, altitudes, and temperatures within the operational limits for UAV use. In flight mechanics, the basic assumption is that the take-off phase consists of two phases (the airborne phase and the ground roll phase), as given in [11]. The ground roll distance can be determined by using the equation (1):

$$s_{LO} = \frac{V_{LO}^2 \cdot m}{2F_{eff}} \ . \tag{1}$$

In equation (1), the force that acts on the UAV (effective/average force) during the take-off phase and the lift-off velocity are estimated by equation (2):

$$V_{LO} = 1.1 \cdot V_{s1} \quad \text{where} \quad V_{s1} = \sqrt{\frac{2 \cdot \dfrac{m \cdot g}{S}}{\rho \cdot C_{z_{\max}}}}$$

and $\tag{2}$

$$F_{eff} = T - \left[F_X + \mu_{tr}(mg - F_Z) \right].$$

The propeller pusher force can be estimated by equation (3):

$$T = \frac{P}{V} \eta_{propeller}. \tag{3}$$

The aerodynamic data presented in the aforementioned equations have been obtained from [12]. This data contains computational fluid dynamics (CFD) analysis of the Tactical UAV model, which includes CFD analysis results of the Tactical UAV in different configurations, ranges of the angle of attack and sideslip angle, and different deflections of control surfaces. The data from [12] has been utilized to obtain a precise estimation of UAV characteristics. Equations from [13, 14] can be used to calculate estimated take-off and landing performance for preliminary analysis.

During the design phase of UAVs, experimental results in the wind tunnel can give more reliable values of aerodynamic characteristics. The main reason why this approach is not utilized is that these experiments are very expensive and time-consuming (the process of preparing the UAV model). Today, the modern approach suggests the usage of numerical methods, such as computational fluid dynamics (CFD) [15-17], to get more accurate estimations of these characteristics. CFD methods provide additional benefits and means to simulate some processes that cannot be replicated in a wind tunnel or solved analytically. CFD methods can be applied to a full scale aircraft or UAV with additional cost (time and computer and software capability). A good example that shows the advantages of CFD and wind tunnels compared to calculation methods is a spin analysis that is given in [18].

Even wind tunnel experiments on models or actual aircraft or UAVs at subsonic speeds could produce three different errors when used for estimation of aerodynamics data. The first is scale effects, the second is the interference effect from wind tunnel walls, and finally, the third is the consequence of errors in the model. Additional information about the aforementioned discussion and the correlation between wind tunnel test data and flight test data is given in [19]. In the diagram (Fig.2), the aerodynamic coefficients of the Tactical UAV in take-off configuration have been obtained from [20].

In the CFD analysis, the propeller effect has not been evaluated. The just-mentioned effects will usually have a negligible contribution to the lift force and a small contribution to the drag force. In order to get a more precise estimation, the drag force coefficient has been increased by 10%. In this manner, the calculation process includes all additional drag (antennas, sensors, tubes, and installations) that are not included during CFD analysis.

The effect of low Reynolds numbers on propeller characteristics is an important consideration during the UAV design process. The effective engine performance characteristics given in [21] with the propeller efficiency factor rated as $\eta_{propeller} = 0.45$ can be used for estimation of power given to the propeller, but additional information must be considered.
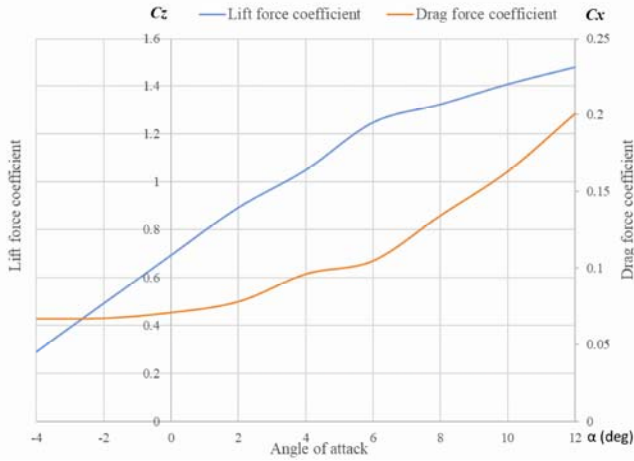
Figure 2. Estimated lift force coefficient and drag force coefficient versus angle of attack for Tactical UAV in take-off configuration [20]

First, it is necessary to determine whether the engine was calibrated or not. If not, the chart may not be applicable to the presented problem. It should be noted that the installation of the engine on the UAV will produce certain losses, known as the thrust deduction factor. The calibrated engine power given by factory charts and the actual engine power on the UAV will not be the same due to this factor. In the presented case, with a pusher propeller, the reduction in propeller thrust can be the result of reduced airflow as the fuselage is in front of the engine, which should be taken into account.

The propeller efficiency is influenced by many factors such as the propeller diameter, the propeller RPM, and true airspeed. If these three parameters are combined into one parameter, the advance ratio can be defined as:

$$J = \frac{V}{ND}. \tag{4}$$

In the previous equation, the N is the propeller rotational speed, D is the propeller diameter, and V is true airspeed. The advance ratio is functionally dependent on the power coefficient. The propeller power coefficient depends on the propeller diameter, propeller rotational speed, air density, as well as the shaft horsepower. On the other hand, the coefficient of absorbed power, C_P, is estimated by equation (5):

$$C_p = \frac{P}{\rho N^3 D^5}. \tag{5}$$

By equation (5) the new non-dimensional parameter is defined, where the ρ stand for air density and P for the shaft horsepower. Additional information about propeller characteristics can be obtained from [22]. As it is well known in the take-off phase, the speed of aircraft or UAVs will increase. The advance ratio will start to increase. The data given in diagram (Fig.3) shows that the propeller performance improves with increasing UAV airspeed during the take-off phase until the maximum airspeed for the designed propeller is reached.

In the diagram (Fig.3) the propeller efficiency is given as a function of the advance ratio. The propeller efficiency given in Fig.3 did not include the ground effect on lift and drag force. For the take-off phase, the advance ratio is estimated as $J \leq 0.31$ and, analysing the data from Fig.3, the propeller efficiency should be in the range of 0.2 to 0.6.
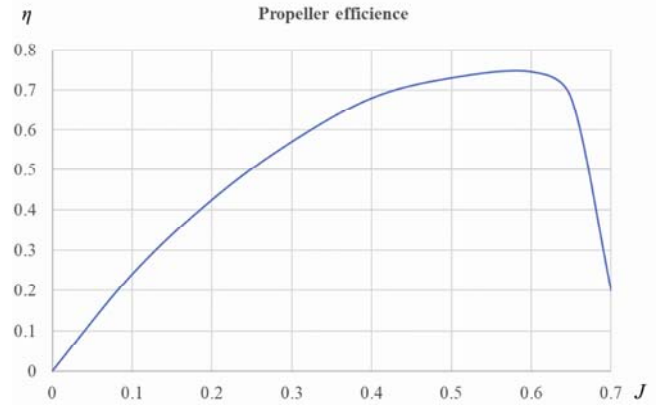

Figure 3. The propeller efficiency vs advance ratio

The maximum force that the propeller could generate is the static propeller force. Consequently, the starting acceleration will be the greatest. The data from the diagram (Fig.4) shows the change in airspeed over time during the take-off phase. Six seconds after the start of the take-off phase, the UAV airspeed is greater than 10 m/s. For the rest of the take-off phase, it can be assumed that the UAV speed is linearly increasing with time, with two different gradients.

In Table 2, the functional dependency of the advance ratio vs. airspeed is given, and the presented results indicate that the propeller efficiency is adequately estimated. The low value of propeller efficiency is strongly influenced by the low value of lift-off speed. For constant-speed propellers and a higher value of lift-off speed, it is reasonable to expect a higher value of propeller efficiency.

Table 2. Propeller advance ratio vs airspeed

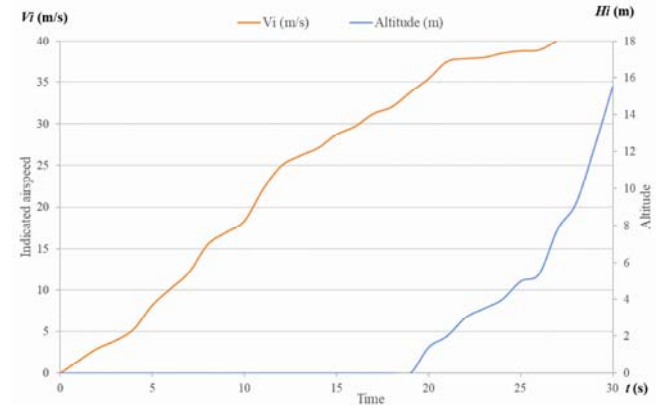| V (m/s)	0	10	20	30	35
V (km/h)	0	36	72	108	126
J	0	0.115	0.231	0.346	0.404

Figure 4. Tactical UAV indicated airspeed and altitude during take-off phase

The average force acting on the UAV during the analyzed flight phase is calculated according to [6], using the average speed of the UAV, which is 70% of V_{LO}. However, it was shown in [23] that assuming constant UAV acceleration at 70% V_{LO} may not always be accurate, as acceleration can vary significantly. In fact, during flight testing of many aircraft and UAVs, it has been observed that take-off acceleration decreases as speed approaches V_{LO}. Therefore, to obtain a more precise estimation of the take-off roll distance, a numerical method should be employed.

In [24], it has been shown that additional analysis should be done for the ground run phase as the propeller slipstream interacts with the ground, which can result in up to a 30% thrust force loss due to the slipstream effect. Well-known data given in [6] shows that the propeller blade angle of attack varies with airspeed and the propeller thrust at the same time, leading to the conclusion that the propeller efficiency is functionally dependent on airspeed. The aforementioned losses in propeller efficiency are caused by the low value of the propeller advance ratio and the low Reynolds number effect during the take-off phase.

The second mentioned part of the take-off phase, where the UAV is airborne and needs to climb to a height of 15 m above the runway, can be evaluated using equation (6):

$$s_A = R \sin \theta_{OB}. \tag{6}$$

In the previous equation, the radius of the curvature path for the take-off phase and the angle θ_{OB} can be estimated using equation (7):

$$R = \frac{6.95 \cdot V_{S1}^2}{g} \quad \text{and} \quad \theta_{OB} = \text{arc}(\cos \theta) = 1 - \frac{15}{R}. \tag{7}$$

The stalling speed in equation (7) is a function of ambient air temperature, altitude, and UAV mass. The take-off distance can be calculated by (8):

$$s_{TO} = s_{LO} + s_A. \tag{8}$$

Landing distance

Landing distance can usually be divided into three segments: ground roll distance, approach distance, and flare distance. During the landing phase, the rate of descent should be reduced to a value not greater than 5 m/s. At a vertical distance of approximately 5 m above the ground, the autopilot should decrease the power and increase the UAV pitch angle. With this command, the UAV should fly level above the ground with decreasing airspeed. In this attitude, the UAV should touch down with the smallest possible rate of descent. The speed above threshold of the UAV should be close to the stalling speed. The approach distance can be estimated by equation (9):

$$s_{AP} = \frac{15 - h_f}{\tan \theta_{AP}}. \tag{9}$$

The glide path angle during the approach phase is determined by regulations [1]. The value should not be greater than $\theta_{AP} \leq 3°$. In the evaluation process, a value of 3° has been used. The altitude of the UAV above the ground at the end of the approach phase is given by equation (10):

$$h_f = R(1 - \sin \theta_{AP}). \tag{10}$$

The radius of curvature, as defined in equation (10), is given by (11):

$$R = \frac{(V_{AP})_{sr}^2}{g(n-1)}. \tag{11}$$

The load factor average value is estimated as **n**=1.2. It is based upon experience and the average approach speed is given by (12):

$$(V_{AP})_{sr} = k \cdot V_{S1}, \, k = 1.15. \tag{12}$$

The flare distance can be estimated by equation (13):

$$s_{FLARE} = R \sin \theta_{AP}. \tag{13}$$

The ground roll is estimated by equation (14):

$$s_{GR} = -\frac{V_{TD}^2 \cdot m}{2F_{eff}} \quad \text{where} \quad V_{TD} = 1.1 \cdot V_{S0}. \tag{14}$$

In order to evaluate the UAV stalling speed the well known equation should be used (15):

$$V_{s0} = \sqrt{\frac{2 \cdot \frac{m \cdot g}{S}}{\rho \cdot C_{z_{max}}}}. \tag{15}$$

The effective force acting on the UAV during the landing phase can be estimated using a well-known equation (16):

$$F_{eff} = -[F_X + \mu_{tr}(mg - F_Z)]. \tag{16}$$

Finally, the landing distance is given by equation (17):

$$s_{LAND} = s_{AP} + s_{FLARE} + s_{GR}. \tag{17}$$

The presented evaluations in this paper have been chosen for their ease of implementation and ability to provide quick and reliable estimations of UAV characteristics. An additional advantage of the presented method is that it can be used to account for altitude effects from sea level to 3048 m, which is a mandatory requirement in regulations. However, it is important to note that temperature can deviate from the standard temperature, as the Earth's atmosphere is constantly changing with time and regionally around the world. Despite these variations, the aircraft industry typically estimates performance using the standard atmosphere model, in which properties only vary with altitude. If nonstandard atmosphere conditions are required, documents [25-26] should be consulted.

The UAV flight testing

The Aviation Safety Agency in Europe and the Federal Aviation Regulations in the USA precisely describe flight test procedures for aircraft. Additional information can be found in the literature [27-29], but will not be covered in this paper. The UAV's characteristics in this study were obtained using a numerical integration technique. The main goal of aviation regulations is to provide procedures and requirements for safe flight operations for aircraft or UAV operators. Thus, the take-off distance is defined as the distance required for the UAV to achieve additional speed and height reserves that are sufficient for safe flight. UAVs must be capable of performing all maneuvers, including safe landing procedures induced by an engine failure. In this analysis, it is assumed that an airspeed margin above the stall speed in a defined UAV configuration and a height of 15 m will assure the desired maneuvering capability. For the landing phase, additional requirements including lateral-directional maneuvers [30-32] need to be considered.

The flight testing was conducted at Ladjevci Airport, located in the city of Kraljevo.

Results of the analysis and discussion

The calculation method presented in this paper, along with the data provided in Table 3, yields estimated results for both take-off and landing distances.

Table 3. Estimated performance of Tactical UAV

| H (m)	m=220 kg		m=265 kg	
	S_{TO} (m)	S_{LAND} (m)	S_{TO} (m)	S_{LAND} (m)
0	385	580	585	615
1000	480	595	765	635
2000	620	615	1045	660
3000	835	640	1525	685

The data presented in this paper were obtained under standard atmospheric conditions and assumed dry concrete/asphalt runways. Flight test results for the Tactical UAV prototype are provided in Table 4 of [33]. To adjust these results to standard atmospheric conditions, the data in [34] should be used for take-off and landing measurements reduction.

Table 4. The flight tests results

H (m)	m=219 kg	
	s_{TO} (m)	s_{LAND} (m)
0	352	652

In the diagram (Fig.5), the airspeed and altitude of the UAV during landing are presented as a function of time. The experimental results for the Tactical UAV prototype are shown in Table 4, and the obtained data from flight tests and estimated results show very good agreement, with a deviation of only 9% to 12.5%. This is an excellent result for preliminary design estimation. The difference in the results could be due to the inability of the method to obtain a 100% accurate value of the effective force acting on the UAV during this maneuver. The overestimation of the take-off length is a consequence of additional safety factors according to [35, 36].

The presented diagram (Fig.4) illustrates the airspeed and altitude of the UAV during the take-off phase, which is controlled by the flight control computer. As indicated in the Fig.4, the UAV starts at a certain altitude (H_i=0 m) and gradually gains altitude until it reaches a height of 15 m above the runway, at which point the take-off phase is considered complete.
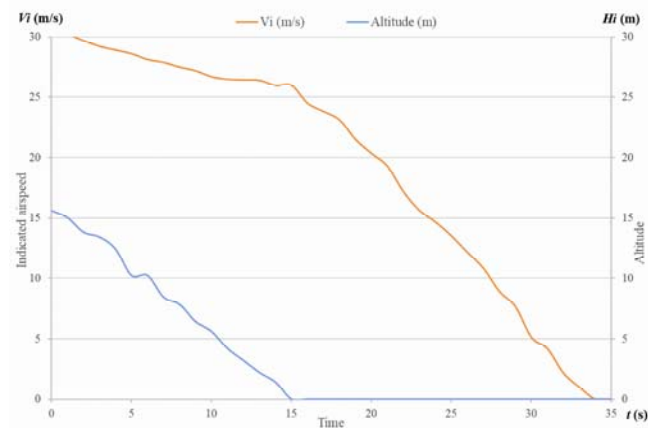
Figure 5. Tactical UAV indicated airspeed and altitude during the landing phase

The presented data in Fig.4 enable the estimation of the function $V_i=f(t)$, which can be used with numerical integration techniques to calculate the take-off distance from the moment the UAV is at rest (0 km/h) to when it reaches a height of 15 m above the runway. To obtain more accurate results, the flight path angle during the airborne phase should also be considered. Using this method, the estimated take-off distance was calculated to be $s_{TO} = 352$ m, showing excellent agreement with the estimated results.

As mentioned in [35], accidents such as collisions with

obstacles, failure to take off, and landing overruns frequently occur in light aircraft and need to be avoided. The purpose of the mentioned documents and articles is to increase awareness of the necessary actions that should ensure that the performance of UAVs or aircraft is adequate. The contribution of factors such as UAV weight, air temperature, wind speed and direction, mud, insects, engine failure, flap settings, ground slope, humidity, etc. on the required runway length for safe take-off and landing is presented in [35]. It was recommended in [35] that safety factors should be used to establish the necessary runway distance, and these factors are originally given in [36].

The estimated minimum required safe runway distance for take-off and landing of the UAV based on the just mentioned factors (1.33 and 1.43) is presented in Table 3. It is important to note that these values are only estimates and the actual required runway distance may vary depending on various factors such as aircraft weight, temperature, wind, runway slope, and more. Therefore, it is recommended that the UAV or aircraft operator consults the Flight Manual and other relevant documents for the specific aircraft or UAV to ensure safe flight operations. Additionally, if there is any doubt about the runway distance requirements, it is advisable to consult with a qualified aviation expert.

Conclusion

In this paper, a procedure for estimating the terminal flight phases of UAVs that require accurate flight-path control, such as take-off and landing performance, has been presented. The analyzed object was the single-engine pusher propeller Tactical UAV developed by the Military Technical Institute (VTI). A method for rapidly estimating the take-off and landing distance has also been provided.

By comparing the calculated data and flight test results it can be concluded that excellent agreement is achieved.

The constant requirements to increase flight safety suggest using safety factors [35-36]. These safety factors can compensate for bad weather conditions, irregular flight control laws, or other factors that can increase the required runway distance.

The results of the presented analysis show that it is possible to accurately predict the take-off and landing characteristics of the medium-altitude long-endurance UAV using CFD results.

References

[1]   STANAG 4671 - *Unmanned aerial vehicle systems airworthiness requirements* (USAR), 2009.

[2]   AEP-80, *Rotary wing unmanned aircraft systems airworthiness requirements*, 2016.

[3]   AEP-83, *Light unmanned aircraft systems airworthiness requirements*, 2014.

[4]   PERKINS,C.D., HAGE,R.E.: *Airplane performance stability and control*, John Wiley& Sons, New York, 1949.

[5]   CHENG,H., GRANDHI,R.V., HANKEY,W.L., BELCHER,P.J.: *Take off and Landing Analysis Methodology for an Airbreathing Space Booster*, Acta Astronautica 1993, Vol.29, No.5, pp. 325-332.

[6]   SNORRI,G.: *General Aviation Aircraft Design: Applied Methods and Procedures*, Elsevier Inc, 2014.

[7]   Vojnotehnički Institut Vojske Srbije 1948-2018, *Monografija VTI*, Beograd, 2018.

[8]   OHME,P.: *A Model-Based Approach to Aircraft Takeoff and Landing Performance Assessment, AIAA Atmospheric Flight Mechanics Conference*, 2009, 10 - 13 August.

[9]   VELIMIROVIĆ,K., VELIMIROVIĆ,N.: *LASTA aircraft with turboprop engine - Determination flight performances, Program*

"Turbolastaperf", 6th International Scientific Conference on Defensive Technologies, OTEH 2014, 09-10. October, Military Technical Institute, Belgrade, SERBIA,, pp. 192-197.

[10] VELIMIROVIĆ,K.,: *Tactical unmanned aerial vehicles equipped with piston engin, determination flight performances*, 2013, Military Technical Institute, Belgrade, SERBIA.

[11] MILENKOVIĆ-BABIĆ,M,, ANTONIĆ,V., PRODIĆ,M., et all., *Aircraft Lasta Take-off and Landing Performance*, Scientific Technical Review, 2019, Vol.69, No.1, pp. 32-38.

[12] B3–600-P-06, *Proračun aerodinamičkih karakteristike taktičke bespilotne letelice srednjeg doleta -PEGAZ*, primenom CFD-a, VTI, Beograd, 2020.

[13] *USAF stability and control DATCOM*, McDonnell Douglas Corporation, Douglas Aircraft Division, 1978.

[14] RAYMER,D.: *Aircraft Design: A Conceptual Approach*, Fifth edition, AIAA education series, 2012.

[15] DEAN,J., CLIFTON,J., BODKIN,D. MORTON,S., MCDANIEL,D.: *Determining the Applicability and Effectiveness of Current CFD Methods in Store Certification Activities*, 48th AIAA Aerospace Sciences Meeting Including the New Horizons Forum and Aerospace Exposition, 4 - 7 January 2010, Orlando, Florida.

[16] KOZIĆ,M.: *Comparison of the Navier-Stokes computations with the experiment for LASTA-95 wing at high angles of attack*, Scientific Technical Review, ISSN 1820-0206, 2006, Vol.56, No.1, pp. 41-44.

[17] DOVATOV,B.: *Primena numeričke dinamike fluida za određivanje uticaja modifikacije zadnjeg dela trupa avona G-4*, 3th International Scientific Conference on Defensive Technologies, OTEH 2009, 08-09. October, Military Technical Institute, Belgrade, SERBIA.

[18] KOZIĆ,M.: *Navier-Stokes Computations and Experimental Comparisonsfor Rudder Efficiency Analysis in the Moderately Steep Spin Part II: Computation Method*, Scientific Technical Review, ISSN 1820-0206, 2018, Vol.68. No.1, pp. 61-65.

[19] BAJOVIĆ,M., VELIMIROVIĆ,K., MOLOVIĆ,V., VELIMIROVIĆ,N.: *The analysis of aerodiynamical coefficient grounded on wind tunnel and flight tests,* 3th International Scientific Conference on Defensive Technologies, OTEH 2009, 08-09. October, Military Technical Institute, Belgrade, SERBIA.

[20] B3–0600–П–06, *Прорачун аеродинамичких карактеристика тактичке беспилотне летелице средњег долета – ПЕГАЗ, применом CFD-а*, VTI, Beograd, 2020.

[21] ZANZOTTERA TECHNOLOGIES SRL, 630HS ENGINE, www.zanzotteraengine.com/engines/630hs-engine/

[22] ROGERS,D.F.: *Propeller Efficiency Rule of Thumb*, American Bonanza Society, 2010.

[23] YECHOUT,T.: *Introduction to Aircraft Flight Mechanics*. AIAA Education Series, 2003.

[24] ALLERTON,D.: *Principles of Flight Simulations*, John Wiley& Sons, 2009.

[25] MIL-HDBK-310. *Global climatic data for developing military products*, June, 1997.

[26] MIL-STD-3013A, *Glossary of definitions, ground rules, and mission profiles to define air vehicle performance capability*, Department of Defense standard practice, September, 2008.

[27] KIMBERLIN,R.: *Flight Testing of Fixed-wing Aircraft*, American Institute of Aeronautics and Astronautics, Virginia, 2003.

[28] CIVIL AVIATION AUTHORITY OF NEW ZELAND, *Take off and Landing Performance*, January, 2011.

[29] PHAK-Chapter 10, *Pilots Handbook of Aeronautical Knowledge,* October, 2008.

[30] STOJAKOVIĆ,P., RAŠUO,B.: *Single propeller airplane minimal flight speed based upon the lateral maneuver condition*, Aerospace Science and Technology. 49 (2016), pp. 239–249.

[31] STOJAKOVIĆ,P., RAŠUO,B.: *Minimal safe speed of the asymmetrically loaded combat airplane*, Aircraft Engineering and Aerospace Technology, 2016, Vol.88, No.1, pp. 42 – 52.

[32] STOJAKOVIĆ,P., VELIMIROVIĆ,K., RAŠUO,B.: *Power optimization of a single propeller airplane take-off run on the basis of lateral maneuver limitations*, Aerospace Science and Technology, 72 (2018), pp. 553-563.

[33] B3–0609–И–06, *Izveštaj o zemaljskim i letnim ispitivanjima letelice*, VTI, Beograd, 2022.

[34] ESDU, *Reduction of take-off and landing measurements to standard conditions*, ESDU Item No. RG 2/1, July 1962 (with Amendments A, April 1987).

[35] Civil Aviation Authority, *Safety sense leaflet 7C aeroplane performance*, January, 2013.

[36] AIC 127/2006. *United Kingdom aeronautical information circular, take-off, climb and landing performance of light aeroplanes*.

Poletno-sletne performanse taktičke bespilotne letelice

Istraživanje predstavljeno u ovom radu prikazuje performanse poletno-sletnih karakteristika jedne Taktičke bespilotne letelice pogonjene potisnom elisom. Sprovedena analiza prikazuje verifikaciju procenjenih proračunskih karakteristika letelice. U ovom radu prikazana je aproksimativna metoda za procenu poletno-sletnih karakteristika bespilotne letelice. Letna ispitivanja su sprovedena kako bi se verifikovale procenjene proračunske vrednosti i postignuta je dobra saglasnost procenjenih i izmerenih rezultata.

Ključne reči: **dužina poletno-sletne staze, bespilotna letelica, letna ispitivanja.**